NANOSCALE ANALYSIS OF PEROVSKITE GRAINS FROM ALLENDE AND AXTELL METEORITES.

T. J. Zega[1,2], V. Manga[2], K. Domanik[1], K. Muralidharan[2], J. Howe[3]. [1]Lunar and Planetary Laboratory, [2]Dept. of Materials Science and Engineering, University of Arizona, Tucson, AZ 85721, USA. [3]Hitachi High-Technologies America Inc., 22610 Gateway Center Drive, Suite 100 Clarksburg, MD 20871. (tzega@lpl.arizona.edu).

Introduction: Calcium-aluminum-rich inclusions (CAIs) are mm- to cm-sized objects that occur in primitive chondritic meteorites. They are composed of minerals that formed at very high temperatures and have radiometric age dates that exceed those of all known solar system materials [1,2]. They are the oldest solar-system objects, and their crystal chemistry and structure can provide clues to the chemical and physical processes that occurred during solar-system formation.

Perovskite, nominally $CaTiO_3$, is an abundant phase within CAIs. It occurs in both the inclusion and the Wark-Lovering rims (WLR) that surround many CAIs [3]. We previously reported on the structure of several perovskite grains from a fluffy type-A CAI in the Allende CV3 chondrite [4]. Here we expand on that work and report additional results from the Allende sample as well as a section from the Axtell CV3 chondrite. This research is part of a broader effort [5] to understand CAI structure and chemistry from the micron scale down to the atomic level and what that tells us about their origins in the early solar system.

Samples and Analytical Methods: Petrographic thin sections of the Allende and Axtell CV3 chondritres were examined using an FEI Helios focused-ion-beam scanning electron microscope (FIB-SEM), equipped with an EDAX energy-dispersive spectrometer (EDS), located at the Lunar and Planetary Laboratory, University of Arizona. Both samples were previously studied in detail by [6]. We acquired backscattered electron (BSE) and EDS spectrum images from local parts of the melilite inclusion and the rim surrounding it.

Based on the imaging and EDS data, several grains from Allende and one from Axtell were chosen for detailed analysis using transmission electron microscopy (TEM). All grains were extracted using the FEI easylift micromanipulator on the Helios and thinned to electron transparency using previously described methods [7]. All samples were ion polished down to 5 keV to remove the amorphous damage layer created by higher-voltage milling.

We analyzed the FIB cross sections using the newly developed 200 keV Hitachi HF5000 TEM. We used the HF5000 located at Hitachi High Technologies (Mito, Japan) and the one currently being installed at the Lunar and Planetary Laboratory, University of Arizona. The HF5000 is equipped with a cold-field-emission gun, an aberration-corrector for scanning TEM (STEM) imaging, a Gatan Quantum image filter (GIF) ER, and a large solid angle Si-drift Oxford EDS system. The HF5000 is capable of rapid (minutes) X-ray mapping of entire FIB sections and atomic-resolution imaging (78 pm).

To complement our experimental work, we performed density-functional theory (DFT) calculations. First-principles DFT calculations were performed with Vienna Ab inito Simulation Package (VASP) using the projector augemented wave method.The goal of these calculations is to investigate the phase transformation energies pertaining to solid solutions relevant to this work, namely perovskite and spinel. Understanding such energies enables quantitative constraints to be placed on the observed micro- and atomic-structures.

Results: BSE imaging shows that localized regions of the Allende and Axtell CV3 chondrites contain abundant perovskite grains. They are typically tens of μm in size with morphologies that range from anhedral to subhedral. In the case of Allende, EDS spectrum imaging reveals a part of the inclusion in which the perovskite is surrounded by abundant hibonite and melilite grains. In Axtel, BSE imaging reveals abundant perovskite grains in the WLR. The perovskites range in size from several to tens of microns and morphologies that range from anhedral to subhedral. Four of the perovskite grains from Allende and one from Axtell were chosen for detailed analysis with TEM. We deposited C straps transecting the perovskite grains and their interfaces with surrounding material.

Bright-field (BF) and dark-field (DF) imaging shows that the FIB sections contain varied degrees of microstructural complexity. The sections are all polyphasic and the perovskite grains hosted within them range in size from nm to several μm with cross-sectional morphologies that range from anhdedral to subhedral. The perovskite grains from three of the Allende samples, 'A', 'B', and 'D' all contain spinel inclusions. Those from 'A' and 'D' measure tens to ~150 nm in size with morphologies that range from anhedral to lathic. The inclusion within section 'C' is relatively larger at 300 × 400 nm. Moreover, it is twinned along the [111] direction. Atomic-scale EDS and electron energy-loss spectroscopy (EELS) show that the V is segregated to atomic columns at the twin boundary and occupy an atomic plane (Fig. 1).

BF and DF TEM imaging of the section from the Axtell CV3 chondrite shows a large (~5 μm) single crystal of perovskite occurs between micron sized grains of melilite, spinel, and a polycrystalline pyroxene. No spinel inclusions were identified within the perovskite grain however, spinel inclusions do occur inside the pyroxene.

Density functional theory was used to predict thermochemical data such as enthalpies of mixing and Gibbs

free energies pertaining to solid solutions of spinel, perovskite etc.). Specifically, the Gibbs free energies as a function of temperature and pressure are calculated, incorporating the finite temperature vibrational contributions to the free energies, from two different approaches; phonon and Debye. The enthalpies of mixing in the solid solutions of various mineral phases are calculated employing Special Quasirandom Structures (SQS). Enthalpies of mixing in $Ca(Ti,V)O_3$ and disordered spinel phases $(Mg,Al)(Mg,Al,V)O_3$ phases are calculated with respect to the binary oxides CaO, TiO_2, VO_2, MgO, Al_2O_3, and V_2O_3. The first-principles predicted data is subsequently used to parametrize the thermodynamic models pertaining to the solid solution phases. DFT calculations were also used to predict the structure of the (111) twins in spinel, and the driving force for the segregation of V segregation at the twin boundaries in stoichiometric spinel.

Discussion: Fluffy type-A CAIs have been inferred to form via condensation in the solar nebula [8]. We did not find evidence of secondary processing in the Allende sample that would argue against condensation. Equilibrium calculations that model a cooling gas of solar composition predict that perovskite will condense at 1593K and 1441K; spinel will condense at 1397K [9]. Thus, one might expect a microstructure consisting of perovskite inside of spinel rather than vice-versa, as we observe here, if the system is experiencing equilibrium condensation.

In a previous report [4], we hypothesized that the solid solution of spinel, containing dissolved V, has an intrinisically higher condensation temperature than that of a solid solution of perovskite. Those calculations are currently underway, but one can assume, based on this hypothesis, that the spinel condensed first as a single crystal at a higher condensation temperature than the perovskite. We note that the high-temperature phase of perovskite is cubic, whereas the lower temperature phase is orthorhombic [10]. We further hypothesize that as temperature of the local system dropped to the condensation temperature of perovskite, the high-temperature cubic form condensed around the spinel. As temperature continued to decrease, the perovskite underwent a displacive phase transition from the cubic to orthorhombic form. This phase transition would have imparted shear stress to the spinel crystal, at which point it became twinned in response to the applied stress. Further, we hypothesize that the V, which was originally homogeneously distributed in the spinel, segregated at the induced twin, driven by an energetically favorable diffusion, forming a plane of atomic columns parallel to the [111] direction. DFT calculations for the segregation of V at twins in different valence states (3^+ and 4^+) are performed. Based on the preliminary 0 K calculations, the segregation of V in a 4^+ valence state seems to unfavorable. The driving force for the segregation in a 3^+ valence state is currently under investigation.

In comparsion, compact type-A CAIs are believed to have experienced partial melting. That we do not find inclusions of spinel within Axtell perovskite may be reflective of its thermal history. If spinel inclusions originally occurred within the perovskite, subsequent annealing or melting could have led to their destruction. We hypothesize that thermal breakdown of any spinel would have depended on its size, the temperature reached, and the duration it was at temperature. Analysis of additional perovskite grains might reveal whether this is a general trend for compact type-A CAIs.

Continued examination of perovskite grains should reveal whether the microstructure we observe here is isolated to those that occur within fluffy type-A CAIs, i.e., those inferred to be nebular condensates or whether it is common to other types of CAIs in CV3 chondrites.

References: [1] Amelin Y. et al. (2002) *Science, 297*, 1678 -1683. [2] Ebel D. S. (2006) *Met. and the Early S. Sys. II,* 253-277. [3] MacPherson G. J. (2004) *T. of Geochem. Volume 1: Met., Comets, and Planet.*, 201-246. [4] Zega T. J. et al. (2016) *LPSC XLVII*, abstract #2807. [5] Bolser D. et al. (2016) *MaPS 51*, 743-756. [6] Simon S.B. (1994) *GCA 58*, 1937-1949. [7] Zega T. J. et al. (2007) *Meteoritics & Planet. Sci., 42,* 1373-1386. [8] MacPherson G. J. and Grossman L. (1984) *Geochim. Cosmochim. Ac., 48,* 29-46. [9] Lodders K. (2003) *Astrophys. J., 591,* 1220-1247. [10] Roushown, A. et al. (2005) *J. of Solid State Chemistry, 178,* 2867-2872.

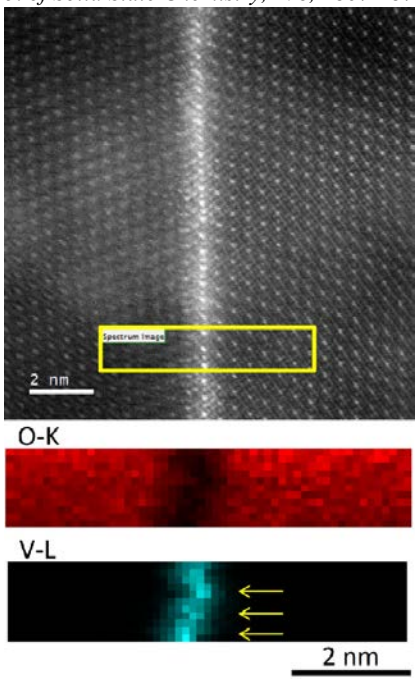

Figure 1. DF atomic-resolution STEM image and O, K and V $L_{2,3}$ maps for a twin boundary within a spinel inclusion in the Allende perovskite grain 'B'.